Research Article | Vol. 24, No. 22 | 31 Oct 2016 | OPTICS EXPRESS 25515

Optics EXPRESS

Theory for voltage modulation of transistor lasers using Franz-Keldysh absorption in the presence of optoelectronic feedback

CHI-HSIANG CHANG,[1,2] SHU-WEI CHANG,[3,4,5] AND CHAO-HSIN WU[1,2,6]

[1]*Graduate Institute of Electronics Engineering, National Taiwan University, Taipei 106, Taiwan*
[2]*Graduate Institute of Photonics and Optoelectronics, National Taiwan University, Taipei 106, Taiwan*
[3]*Research Center for Applied Sciences, Academia Sinica, Nankang, Taipei 11529, Taiwan*
[4]*Department of Photonics, National Chiao-Tung University, Hsinchu 30010, Taiwan*
[5]*swchang@sinica.edu.tw*
[6]*chaohsinwu@ntu.edu.tw*

Abstract: Compared with typical diode lasers (DLs), transistor lasers (TLs) support not only current-controlled but also voltage-controlled modulation. In this work, we theoretically investigate the small-signal voltage modulation of TLs based on the Franz-Keldysh (F-K) absorption and related optoelectronic feedback. In addition to the conventional rate equations relevant to DLs, our model physically includes various F-K effects. An optically induced current due to the F-K absorption may dramatically alter the voltage response of TLs. A model composed of the intrinsic optical response and an electrical transfer function which is fed back by this optical response is proposed to explain the true behaviors of voltage modulation in TLs.

© 2016 Optical Society of America

OCIS codes: (250.5960) Semiconductor lasers; (250.5590) Quantum-well, -wire and -dot devices; (230.0250) Optoelectronics.

References and links

1. J.-S. Youn, M.-J. Lee, K.-Y. Park, H. Rücker, and W.-Y. Choi, "SNR characteristics of 850-nm OEIC receiver with a silicon avalanche photodetector," Opt. Express **22**(1), 900–907 (2014).
2. M. Feng, N. Holonyak, Jr., and W. Hafez, "Light-emitting transistor: Light emission from InGaP/GaAs heterojunction bipolar transistors," Appl. Phys. Lett. **84**(1), 151–153 (2004).
3. M. Feng, N. Holonyak, Jr., and R. Chan, "Quantum-well-base heterojunction bipolar light-emitting transistor," Appl. Phys. Lett. **84**(11), 1952–1954 (2004).
4. G. Walter, C. H. Wu, H. W. Then, M. Feng, and N. Holonyak, Jr., "4.3 GHz optical bandwidth light emitting transistor," Appl. Phys. Lett. **94**(24), 241101 (2009).
5. Z. Duan, W. Shi, L. Chrostowski, X. Huang, N. Zhou, and G. Chai, "Design and epitaxy of 1.5 microm InGaAsP-InP MQW material for a transistor laser," Opt. Express **18**(2), 1501–1509 (2010).
6. W. Huo, S. Liang, C. Zhang, S. Tan, L. Han, H. Xie, H. Zhu, and W. Wang, "Fabrication and characterization of deep ridge InGaAsP/InP light emitting transistors," Opt. Express **22**(2), 1806–1814 (2014).
7. M. Shirao, T. Sato, N. Sato, N. Nishiyama, and S. Arai, "Room-temperature operation of npn- AlGaInAs/InP multiple quantum well transistor laser emitting at 1.3-μm wavelength," Opt. Express **20**(4), 3983–3989 (2012).
8. C. H. Chen, M. Hargis, J. M. Woodall, M. R. Melloch, J. S. Reynolds, E. Yablonovitch, and W. Wang, "GHz bandwidth GaAs light-emitting diodes," Appl. Phys. Lett. **74**(21), 3140–3142 (1999).
9. J. Heinen, W. Hurber, and W. Harth, "Light-emitting diodes with a modulation bandwidth of more than 1 GHz," Electron. Lett. **12**(21), 553–554 (1976).
10. Y.-W. Chern, C.-H. Chang, and C.-H. W. Wu, "The effect of voltage-dependent charge-removing mechanism on the optical modulation bandwidths of light-emitting transistors," IEEE Trans. Electron Dev. **62**(12), 4076–4081 (2015).
11. G. Walter, N. Holonyak, Jr., M. Feng, and R. Chan, "Laser operation of a heterojunction bipolar light-emitting transistor," Appl. Phys. Lett. **85**(20), 4768 (2004).
12. F. Tan, R. Bambery, M. Feng, and N. Holonyak, Jr., "Transistor laser with simultaneous electrical and optical output at 20 and 40 Gb/s data rate modulation," Appl. Phys. Lett. **99**(6), 061105 (2011).
13. H.-L. Wang, Y.-H. Huang, G.-S. Cheng, S. W. Chang, and C.-H. Wu, "Analysis of tunable internal loss caused by Franz–Keldysh absorption in transistor lasers," IEEE J. Sel. Top. Quantum Electron. **21**(6), 270–276 (2015).
14. A. James, N. Holonyak, M. Feng, and G. Walter, "Franz–Keldysh photon-assisted voltage-operated switching of a transistor laser," IEEE Photonics Technol. Lett. **19**(9), 680–682 (2007).

#275175 http://dx.doi.org/10.1364/OE.24.025515
Journal © 2016 Received 7 Sep 2016; revised 12 Oct 2016; accepted 18 Oct 2016; published 24 Oct 2016

Optics EXPRESS

15. M. Feng, N. Holonyak, Jr., H. W. Then, C. H. Wu, and G. Walter, "Tunnel junction transistor laser," Appl. Phys. Lett. **94**(4), 041118 (2009).
16. K. Kudo, K. Yashiki, T. Sasaki, Y. Yokoyama, K. Hamamoto, T. Morimoto, and M. Yamaguchi, "1.55-μm wavelength-selectable microarray DFB-LD's with monolithically integrated MMI combiner, SOA, and EA-Modulator," IEEE Photonics Technol. Lett. **12**(3), 242–244 (2000).
17. N. H. Zhu, H. G. Zhang, J. W. Man, H. L. Zhu, J. H. Ke, Y. Liu, X. Wang, H. Q. Yuan, L. Xie, and W. Wang, "Microwave generation in an electro-absorption modulator integrated with a DFB laser subject to optical injection," Opt. Express **17**(24), 22114–22123 (2009).
18. A. James, G. Walter, M. Feng, and N. Holonyak, Jr., "Photon-assisted breakdown, negative resistance, and switching in a quantum-well transistor laser," Appl. Phys. Lett. **90**(15), 152109 (2007).
19. L. A. Coldren, S. W. Corzine, and M. L. Mashanovitch, *Diode Lasers and Photonic Integrated Circuits* (John Wiley and Sons, 2012).
20. K. Tharmalingam, "Optical absorption in the presence of a uniform field," Phys. Rev. **130**(6), 2204–2206 (1963).
21. P. Baureis, "Compact modeling of electrical, thermal and optical LED behavior," in *Proceedings of 35th European IEEE Solid-State Device Research Conference* (2005).
22. H.-L. Wang, Y.-J. Huang, and C.-H. Wu, "Optical frequency response analysis of light-emitting transistors under different microwave configurations," Appl. Phys. Lett. **103**(5), 051110 (2013).
23. H. W. Then, M. Feng, and N. Holonyak, Jr., "Microwave circuit model of the three-port transistor laser," J. Appl. Phys. **107**(9), 094509 (2010).
24. H.-L. Wang, P.-H. Chou, and C.-H. Wu, "Microwave determination of quantum-well capture and escape time in light-emitting transistors," IEEE Trans. Electron Dev. **60**(3), 1088–1091 (2013).
25. M. Feng, J. Qiu, C. Y. Wang, and N. Holonyak, Jr., "Intra-cavity photon-assisted tunneling collector-base voltage-mediated electron-hole spontaneous-stimulated recombination transistor laser," J. Appl. Phys. **119**(8), 084502 (2016).

1. Introduction

As developments of technology and information circulation grow rapidly, optoelectronic integrated circuits (OEICs) become more important [1], and therefore the more attention is drawn to the high speed optoelectronic devices nowadays. The light-emitting transistor (LET) based on heterostructures of the indium gallium phosphide/gallium arsenide (InGaP/GaAs) material was first proposed by Feng and Holonyak in 2004 [2,3]. With both the high-speed features of heterojunction bipolar transistors (HBTs) and efficient radiative recombination of carriers in quantum wells (QWs), a modulation bandwidth of LETs as high as 4.3 GHz has been demonstrated in the regime of spontaneous emissions [4]. In addition to InGaP/GaAs, different material systems such as the indium-phosphide (InP) family which is utilized in the telecommunication were proposed and fabricated [5–7]. These unique three-port devices have great potential for future optical interconnects and OEICs.

The optical response of LETs is faster than that of conventional diode lasers (DLs) [8,9] due to a heavily doped base and transistor structure [10]. Furthermore, after the redesign of layouts and introduction of cavities for photon storage, LETs can be turned into transistor lasers (TLs) [11]. It has been shown previously that TLs could exhibit a high modulation bandwidth capable of data transmissions at 40 Gb/s [12]. As TLs are operated in the forward-active mode, the junction between the emitter and base (EB junction) is forward biased while that between the base and collector (BC junction) is reversely biased. The significant electric field in the BC junction induces additional absorption for the photons generated in the active region even though the photon energy is less than the bandgap energy of the reversely biased junction. This phenomenon is known as the Franz-Keldysh (F-K) absorption or photon-assisted tunneling. With the F-K effect in BC junctions [13], the voltage-controlled modulation of TLs becomes plausible in addition to the current-controlled modulation of typical DLs. The optical responses due to the voltage modulation are relatively flat in the experiment [14,15], which is beneficial from a system point of view. In this way, external voltage-controlled modulators which are designed for conventional devices may not be required for TLs [16,17].

In this work, the effect of F-K absorption on the voltage modulation of TLs is investigated. Due to the F-K absorption in the BC junction, the mechanism of breakdowns is enhanced in TLs [18]. To understand the dynamics and optical responses of TLs, we

Optics EXPRESS

incorporate the F-K effect into conventional rate equations which describe the modulation characteristics of DLs. Based on the models of rate equations and F-K absorption [19,20], new terms related to the F-K effect are introduced into the rate equations. The theoretical results of direct-current (DC) and small-signal alternating-current (AC) characteristics of optical responses are both investigated. While the DC characteristics look physical, the intrinsic optical AC response of TLs under the F-K voltage modulation exhibits an enhancement peak of about 25 dB, which is scarcely observed in pervious experiment. In fact, apart from the intrinsic optical response, an electrical model that incorporates parasitic resistances, capacitances, and inductances should be considered in the overall small-signal analysis. The measured optical response does depend on these parasitic elements. These analytical techniques are often adopted for light-emitting diodes (LEDs) or LETs [21,22]. In our case of TLs, a theoretical model composed of the intrinsic optical response and an electrical transfer function which is fed back by this optical response is proposed to elucidate the true behavior of voltage modulation in TLs. The giant AC peak disappears at measurement probes through this optoelectronic feedback. With the rate equations in which the FK effect is built and the electrical transfer function taken into account, the overall voltage-controlled optical modulation response of TLs is explained.

This paper is organized as follows. The device structure and results of the DC model are presented in section 2. The small-signal analysis and results are demonstrated in section 3. In section 4, we present the complete model which describes the characteristics of voltage-controlled modulations for TLs. The conclusion is given in section 5.

2. Device structure and rate equations with Franz-Keldysh absorption

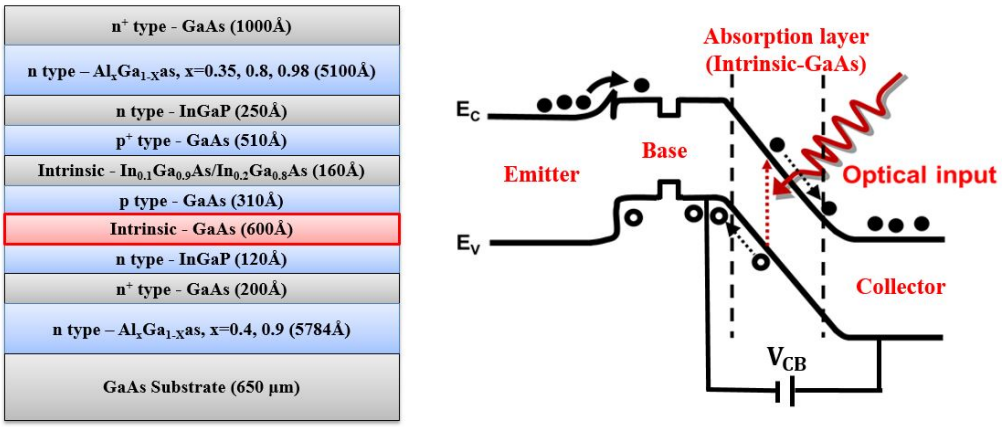

Fig. 1. The layer structure and band diagram of the TL. A QW is incorporated in the p-type base for photon emissions. The additional holes generated by the F-K absorption flow back into the base (active) region and participate in the carrier-photon interaction.

The layer structure of the device considered in this study is shown schematically in Fig. 1(a). It consists of a 3000 Å n-type doped GaAs buffer layer, followed by a 634 Å n-type $Al_{0.4}Ga_{0.6}As$ layer, a 5000 Å n-type $Al_{0.9}Ga_{0.1}As$ layer, and a 150 Å n-type $Al_{0.4}Ga_{0.6}As$ layer, which form the bottom cladding layer as a whole (5784 Å in total). These layers are then followed by a 200 Å n-type sub-collector layer which is heavily doped for collector contact, a 120 Å $In_{0.49}Ga_{0.51}P$ etch stop layer, a 600 Å undoped GaAs collector layer, and a 980 Å p-type GaAs base layer which contains a 160 Å InGaAs QW as the active region. The epitaxial structure is completed with the growth of a 250 Å n-type $In_{0.49}Ga_{0.51}P$ emitter layer, and a 5100 Å n-type $Al_xGa_{1-x}As$ (x = 0.35, 0.8, and 0.98) layer for the current-confinement aperture. Finally, a 1000 Å n-type GaAs layer which is heavily doped for emitter contact is deposited on the top. The emission range of the QW is around 980 nm.

Optics EXPRESS

As illustrated in Fig. 1(b), the 600 Å intrinsic GaAs layer between the base and collector function as a heterojunction phototransistor (HPT) during the voltage-controlled modulation. In the presence of the F-K absorption due to the reverse bias of the BC junction, the photons emitted from the QW are absorbed and generate additional electron-hole pairs in the region of intrinsic GaAs. These electron-hole pairs are then split by the electric field with electrons and holes flowing into the collector and base (active) region, respectively. The holes injected into the base may then participate in the carrier-photon interaction again.

In the presence of F-K absorption in the BC junction, the conventional rate equations of carrier and photon densities in DLs need to be modified. The generalized rate equations are

$$\frac{\mathrm{d}N}{\mathrm{d}t} = \frac{\eta_{\mathrm{i}} i_{\mathrm{B}}}{eV_{\mathrm{a}}} - R - v_{\mathrm{g}} g N_{\mathrm{p}} + \eta_{\mathrm{BC}} \frac{\Gamma_{J_{\mathrm{BC}}}}{\Gamma_{\mathrm{a}}} v_{\mathrm{g}} \alpha N_{\mathrm{p}}, \tag{1a}$$

$$\frac{\mathrm{d}N_{\mathrm{p}}}{\mathrm{d}t} = \left(\Gamma_{\mathrm{a}} v_{\mathrm{g}} g - \frac{1}{\tau_{\mathrm{p}}} \right) N_{\mathrm{p}} + \Gamma_{\mathrm{a}} \beta_{\mathrm{sp}} R_{\mathrm{sp}} - \Gamma_{J_{\mathrm{BC}}} v_{\mathrm{g}} \alpha N_{\mathrm{p}}, \tag{1b}$$

where N and N_{p} are the minority carrier (electron) and photon densities, respectively; η_{i} is the injection efficiency; i_{B} is the base current; e is the electron charge; V_{a} is the volume of active region; R is the carrier recombination rate and is modeled as the spontaneous emission rate $R_{\mathrm{sp}} = N/\tau_{\mathrm{sp}}$ parameterized by a lifetime τ_{sp} which depends on the p-type doping level in the base (non-radiative recombination is not considered here); v_{g} is the group velocity; $g = a_0(N - N_{\mathrm{tr}})/(1 + \varepsilon N_{\mathrm{p}})$ is the optical gain for which the linear gain model parameterized by the differential gain a_0, transparency carrier density N_{tr}, and gain compression factor ε is adopted; η_{BC} is the injection efficiency of the hole current from the collector to base; Γ_{a} and $\Gamma_{J_{\mathrm{BC}}}$ are the confinement factors of the active region and BC junction, respectively; α is the absorption coefficient due to the F-K effect; τ_{p} is the photon lifetime; β_{sp} is the spontaneous emission coupling factor defined as the percentage of the total spontaneous emissions coupled into the lasing mode. In these two rate equations, we adopt the formula of F-K absorption coefficient α in [20], which has the following analytical form:

$$\alpha \propto \sqrt{\hbar\theta_{\mathrm{F}}} \left\{ -\eta \mathrm{Ai}^2(\eta) + [\mathrm{Ai}'(\eta)]^2 \right\}, \tag{2a}$$

$$\eta = \frac{E_{\mathrm{g}} - \hbar\omega_{\mathrm{p}}}{\hbar\theta_{\mathrm{F}}}, \quad \theta_{\mathrm{F}} = \left(\frac{eF}{\sqrt{2\mu\hbar}} \right)^{2/3}, \tag{2b}$$

where $\mathrm{Ai}(\eta)$ and $\mathrm{Ai}'(\eta)$ are Airy function of the first kind and its derivative, respectively; E_{g} (1.421 eV) and $\hbar\omega_{\mathrm{p}}$ (1.265 eV) are energies corresponding to the bandgap of intrinsic GaAs and lasing mode, respectively; μ is the reduced mass of electron-hole pairs; F is the electric field between the base and collector; and $\hbar$ is Planck's constant. In the DC bias condition, the electric field F is approximately the ratio between the voltage drop V_{CB} between the C and B terminals and thickness d of intrinsic GaAs in the BC junction, namely, $F = V_{\mathrm{CB}}/d$. We note that the last term $\Gamma_{J_{\mathrm{BC}}} v_{\mathrm{g}} \alpha N_{\mathrm{p}}$ in Eq. (1b) is the modal absorption rate due to the F-K effect in the BC junction. A similar term $\eta_{\mathrm{BC}}(\Gamma_{J_{\mathrm{BC}}}/\Gamma_{\mathrm{a}}) v_{\mathrm{g}} \alpha N_{\mathrm{p}}$ in Eq. (1a) corresponds to the additional electrons (minority carriers) from the emitter side

Optics EXPRESS

which balance the holes generated by the F-K absorption and injected into the active region. Numerical values of the parameters utilized in later calculations are listed in Table 1. The two confinement factors Γ_a and $\Gamma_{J_{BC}}$ are estimated from the layer structure in Fig. 1 with commercial mode solver of waveguides. Others related to the gain medium (a_0 and N_{tr}) are adjusted from those of the similar material system in [19], taking into account that the preexisting holes are present in the QW due to the heavily p-doped base. A lifetime τ_{sp} in the sub-nanosecond rather nanosecond range is adopted for TL here since the threshold current density of TLs is usually a few times higher than that of commercial DLs. This choice of τ_{sp} is also consistent with the higher modulation bandwidth of TLs than that of DLs [12].

Table 1. List of parameters for TLs.

	η_i	V_a	τ_{sp}	a_0
Value	0.8	$16.08\,(\mu m^3)$	200 (ps)	$6.1\times10^{-20}\,(m^2)$
	η_{BC}	$\Gamma_{J_{BC}}$	Γ_a	v_g
Value	0.8	0.3659	0.074481	$7.5\times10^{7}\,(m\,s^{-1})$
	N_{tr}	ε	τ_p	β_{sp}
Value	$7\times10^{23}\,(m^{-3})$	$1.5\times10^{-23}\,(m^3)$	2.15 (ps)	8.69×10^{-5}

The TL is operated in the common-emitter configuration. The voltage drop V_{CB} changes the absorption coefficient α . The DC light-versus-current-voltage (LIV) and carrier-density-versus-current-voltage family curves are self-consistently solved from Eqs. (1a) and (1b) by setting the time derivatives of N and N_p to zero (steady state) at a given i_B and V_{CB} . Figure 2(a) shows the LIV family curves of the TL. The threshold current increases with V_{CB} since the larger reverse bias results in the more significant F-K absorption and hence the fewer photons and output power in the lasing mode. Meanwhile, the collector current i_C at a high reverse bias of V_{CB} would also increase as a result of the additional electrons generated from the F-K absorption. The simulated LIV curves show great consistency with the experimental results presented by Feng et al [25]. The F-K absorption and corresponding photon-assisted tunneling feedback current will play an important role in determinations of DC performance as well as AC frequency response of TLs. The carrier density N in the active region as a function of i_B and V_{CB} is shown in Fig. 2(b). For DLs, the carrier density is pinned at a certain value once the threshold condition is reached. This phenomenon is also present in TLs. As the voltage V_{CB} increases, this threshold carrier density is raised, in accordance with the power drop on the LIV family curves. At a fixed i_B, as the voltage V_{CB} exceeds certain critical value, the device would not lase anymore and just turns into a spontaneous-emission source.

3. Small-signal analysis

After the DC bias condition is determined, we then look into the small-signal analysis of the voltage-controlled modulation. For a generic variable X , we write it as $X = X^{(0)} + \Delta X$, where $X^{(0)}$ and ΔX are the DC component and small deviation of X . In order to monitor the dynamics in the response of TLs, we carry out the expansion of various variables in Eqs. (1a) and (1b) around their biased points but only keep the perturbation up to the first order. In this way, Eqs. (1a) and (1b) are transformed into

Optics EXPRESS

$$\frac{\mathrm{d}\Delta N}{\mathrm{d}t} = -\Delta R_{\mathrm{sp}} - v_{\mathrm{g}}\Delta g N_{\mathrm{p}}^{(0)} + v_{\mathrm{g}} g^{(0)}\Delta N_{\mathrm{p}} + \eta_{\mathrm{BC}}\frac{\Gamma_{J_{\mathrm{BC}}}}{\Gamma_a}\left(v_{\mathrm{g}}\Delta\alpha N_{\mathrm{p}}^{(0)} + v_{\mathrm{g}}\alpha^{(0)}\Delta N_{\mathrm{p}}\right), \quad (3a)$$

$$\frac{\mathrm{d}\Delta N_{\mathrm{p}}}{\mathrm{d}t} = \Gamma_{\mathrm{a}} v_{\mathrm{g}}\Delta g N_{\mathrm{p}}^{(0)} + \Gamma_{\mathrm{a}} v_{\mathrm{g}} g^{(0)}\Delta N_{\mathrm{p}} - \frac{\Delta N_{\mathrm{p}}}{\tau_{\mathrm{p}}} - \Gamma_{J_{\mathrm{BC}}} v_{\mathrm{g}}\Delta\alpha N_{\mathrm{p}}^{(0)} - \Gamma_{J_{\mathrm{BC}}} v_{\mathrm{g}}\alpha^{(0)}\Delta N_{\mathrm{p}} + \Gamma_{\mathrm{a}}\Delta(\beta_{\mathrm{sp}} R_{\mathrm{sp}}), \quad (3b)$$

where Δi_{B} is set to zero in absence of the current-controlled modulation.

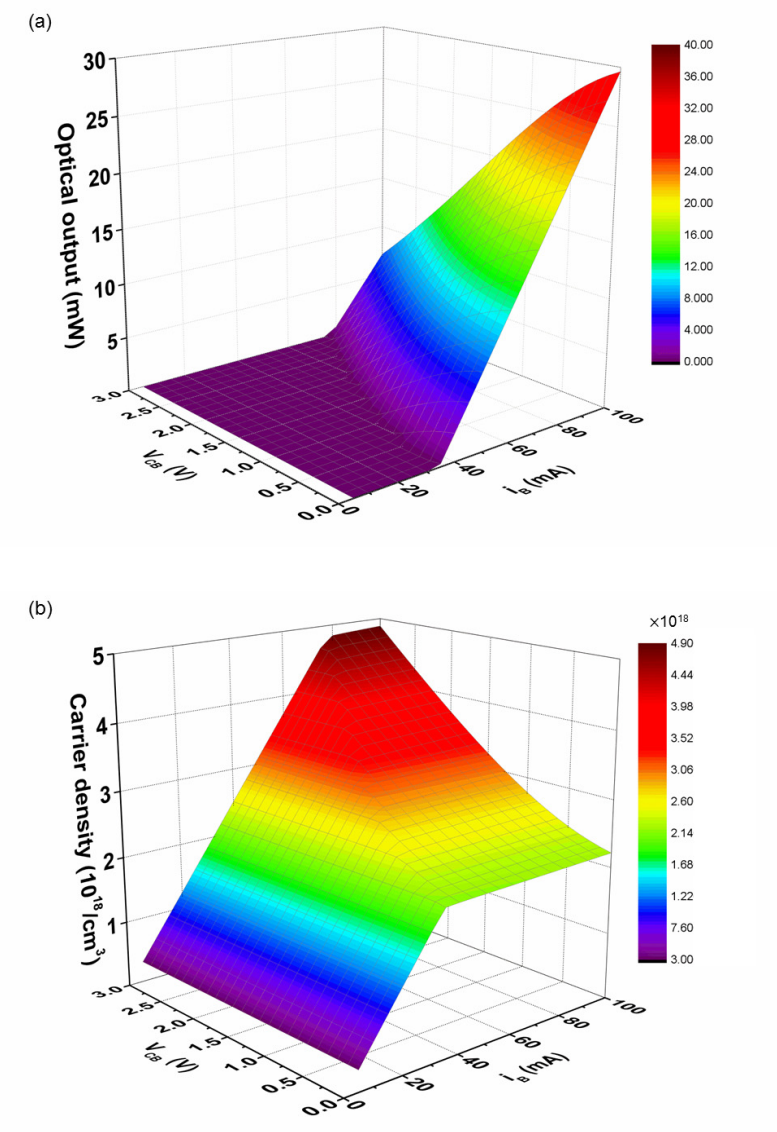

Fig. 2. (a) The LIV family curves of the TL. The more significant F-K absorption at the larger V_{CB} makes the light output turns smaller. (b) The carrier density versus i_{B} and V_{CB}. At a fixed i_{B}, if V_{CB} is larger than a critical value, the device would not lase anymore and turn into a spontaneous-emission source.

Optics EXPRESS

In TLs, the p-type base is heavily doped, which brings about preexisting holes in the QW. Under such circumstances, the density of holes in the QW and therefore the lifetime τ_{sp} does not vary much during small-signal modulations. In this way, we may approximate ΔR_{sp} as $\Delta N / \tau_{sp}$. Typically, the last term on the right-hand side of Eq. (3b) is small compared with others in conventional DLs, and we would simply drop it. The gain variation Δg can be expanded by both carrier and photon densities as

$$\Delta g = a\Delta N - a_p \Delta N_p, \tag{4a}$$

$$a = \left.\frac{\partial g}{\partial N}\right|_{N=N^{(0)}, N_p=N_p^{(0)}} = \frac{a_0}{1+\varepsilon N_p^{(0)}}, \tag{4b}$$

$$a_p = -\left.\frac{\partial g}{\partial N_p}\right|_{N=N^{(0)}, N_p=N_p^{(0)}} = \frac{\varepsilon g^{(0)}}{1+\varepsilon N_p^{(0)}}. \tag{4c}$$

Also, the absorption variation $\Delta\alpha$ is proportional to ΔF through a constant K defined as

$$\Delta\alpha = K\Delta F, \quad K = \frac{\alpha^{(0)}}{3F^{(0)}}\left\{\frac{\eta^{(0)}\mathrm{Ai}^2(\eta^{(0)}) + [\mathrm{Ai}'(\eta^{(0)})]^2}{-\eta^{(0)}\mathrm{Ai}^2(\eta^{(0)}) + [\mathrm{Ai}'(\eta^{(0)})]^2}\right\}. \tag{5}$$

We then substitute Δg in Eq. (4a) into Eqs. (3a) and (3b) and rewrite the two rate equations in the matrix form as

$$\frac{\mathrm{d}}{\mathrm{d}t}\begin{pmatrix}\Delta N\\ \Delta N_p\end{pmatrix} = \begin{pmatrix}-\gamma_{NN} & -\gamma_{NP}\\ \gamma_{PN} & -\gamma_{PP}\end{pmatrix}\begin{pmatrix}\Delta N\\ \Delta N_p\end{pmatrix} + \begin{pmatrix}\gamma_{N\alpha}\Delta\alpha\\ -\gamma_{P\alpha}\Delta\alpha\end{pmatrix}, \tag{6}$$

where various matrix elements (coupling factors) are

$$\gamma_{NN} \equiv \frac{1}{\tau_{sp}} + v_g a N_p^{(0)}, \quad \gamma_{NP} \equiv v_g g^{(0)} - v_g a_p N_p^{(0)} - \eta_{BC}\frac{\Gamma_{J_{BC}}}{\Gamma_a} v_g \alpha^{(0)}, \quad \gamma_{N\alpha} \equiv \eta_{BC}\frac{\Gamma_{J_{BC}}}{\Gamma_a} v_g N_p^{(0)},$$

$$\gamma_{PN} \equiv v_g a \Gamma_a N_p^{(0)}, \quad \gamma_{PP} \equiv v_g a_p \Gamma_a N_p^{(0)} - \Gamma_a v_g g^{(0)} + \frac{1}{\tau_p} + \Gamma_{J_{BC}} v_g \alpha^{(0)}, \quad \gamma_{P\alpha} \equiv \Gamma_{J_{BC}} v_g N_p^{(0)}. \tag{7}$$

With a sinusoidal modulation of voltage ΔV_{CB}, various responses are also sinusoidal. In this case, we may write the solution of a generic variation ΔX as $\Delta X = \mathrm{Re}[X_1 \exp(j\omega t)]$, where X_1 is the amplitude of the modulation; and ω is the modulation frequency. In the sinusoidal steady state, the time derivative $\mathrm{d}/\mathrm{d}t$ gives rise to the factor $j\omega$ for various amplitudes X_1, and Eq. (6) can be rearranged as

$$\begin{pmatrix}\gamma_{NN} + j\omega & \gamma_{NP}\\ -\gamma_{PN} & \gamma_{PP} + j\omega\end{pmatrix}\begin{pmatrix}N_1\\ N_{p,1}\end{pmatrix} = \begin{pmatrix}\gamma_{N\alpha}\alpha_1\\ -\gamma_{P\alpha}\alpha_1\end{pmatrix}. \tag{8}$$

The small-signal carrier and photon densities then can be obtained by inverting the matrix at the left-hand side of Eq. (8). Their expressions are shown as follows:

$$N_1 = \frac{H(\omega)\left[(\gamma_{PP} + j\omega)\gamma_{N\alpha} + \gamma_{NP}\gamma_{P\alpha}\right]}{\omega_R^2}\alpha_1, \tag{9a}$$

Optics EXPRESS

$$N_{\mathrm{p},1}=\frac{H(\omega)\left[-(\gamma_{\mathrm{NN}}+j\omega)\gamma_{\mathrm{P}\alpha}+\gamma_{\mathrm{N}\alpha}\gamma_{\mathrm{PN}}\right]}{\omega_{\mathrm{R}}^2}\alpha_1, \tag{9b}$$

where the transfer function $H(\omega)$ is featured by the relaxation resonance frequency ω_{R} ad damping factor γ as

$$H(\omega)\equiv\frac{\omega_{\mathrm{R}}^2}{\Delta}=\frac{\omega_{\mathrm{R}}^2}{\omega_{\mathrm{R}}^2-\omega^2+j\omega\gamma},\qquad \Delta=\gamma_{\mathrm{NN}}\gamma_{\mathrm{PP}}+\gamma_{\mathrm{NP}}\gamma_{\mathrm{PN}}+j\omega(\gamma_{\mathrm{NN}}+\gamma_{\mathrm{PP}})-\omega^2, \tag{10a}$$

$$\begin{aligned}\omega_{\mathrm{R}}^2&=\gamma_{\mathrm{NP}}\gamma_{\mathrm{PN}}+\gamma_{\mathrm{NN}}\gamma_{\mathrm{PP}}\\&=\left(v_{\mathrm{g}}g^{(0)}-v_{\mathrm{g}}a_{\mathrm{p}}N_{\mathrm{p}}^{(0)}-\eta_{\mathrm{BC}}\frac{\Gamma_{\mathrm{J_{BC}}}}{\Gamma_{\mathrm{a}}}v_{\mathrm{g}}\alpha^{(0)}\right)v_{\mathrm{g}}a\Gamma_{\mathrm{a}}N_{\mathrm{p}}^{(0)}\\&+\left(\frac{1}{\tau_{\mathrm{sp}}}+v_{\mathrm{g}}aN_{\mathrm{p}}^{(0)}\right)\left(v_{\mathrm{g}}a_{\mathrm{p}}\Gamma_{\mathrm{a}}N_{\mathrm{p}}^{(0)}-\Gamma_{\mathrm{a}}v_{\mathrm{g}}g^{(0)}+\frac{1}{\tau_{\mathrm{p}}}+\Gamma_{\mathrm{J_{BC}}}v_{\mathrm{g}}\alpha^{(0)}\right),\end{aligned} \tag{10b}$$

$$\gamma=\gamma_{\mathrm{NN}}+\gamma_{\mathrm{PP}}=\frac{1}{\tau_{\mathrm{sp}}}+v_{\mathrm{g}}aN_{\mathrm{p}}^{(0)}+v_{\mathrm{g}}a_{\mathrm{p}}\Gamma_{\mathrm{a}}N_{\mathrm{p}}^{(0)}-\Gamma_{\mathrm{a}}v_{\mathrm{g}}g^{(0)}+\frac{1}{\tau_{\mathrm{p}}}+\Gamma_{\mathrm{J_{BC}}}v_{\mathrm{g}}\alpha^{(0)}. \tag{10c}$$

The relaxation resonance frequency ω_{R} and damping factor γ in Eqs. (10b) and (10c) are different from those of conventional DLs [19] since they include the new terms from the F-K effect in the BC junction. By utilizing the expression of $\Delta\alpha$ in Eq. (5) for α_1 and defining an effective voltage amplitude $V_1\equiv F_1 d$ which is close to $V_{\mathrm{CB},1}$ at low frequencies, the ratio between the variation $N_{\mathrm{p},1}$ of photon density and effective voltage V_1, which is defined as $T_{\mathrm{p}}(\omega)$, can be derived as

$$T_{\mathrm{p}}(\omega)\equiv\frac{N_{\mathrm{p},1}}{V_1}=\frac{\left[v_{\mathrm{g}}a\Gamma_{\mathrm{a}}N_{\mathrm{p}}^{(0)}\eta_{\mathrm{BC}}\frac{\Gamma_{\mathrm{J_{BC}}}}{\Gamma_{\mathrm{a}}}v_{\mathrm{g}}N_{\mathrm{p}}^{(0)}\left(j\omega+\frac{1}{\tau_{\mathrm{sp}}}+v_{\mathrm{g}}aN_{\mathrm{p}}^{(0)}\right)^{-1}-\Gamma_{\mathrm{J_{BC}}}v_{\mathrm{g}}N_{\mathrm{p}}^{(0)}\right]K}{\left[\begin{aligned}&j\omega-v_{\mathrm{g}}a\Gamma_{\mathrm{a}}N_{\mathrm{p}}^{(0)}\left(v_{\mathrm{g}}a_{\mathrm{p}}N_{\mathrm{p}}^{(0)}-v_{\mathrm{g}}g^{(0)}+\eta_{\mathrm{BC}}\frac{\Gamma_{\mathrm{J_{BC}}}}{\Gamma_{\mathrm{a}}}v_{\mathrm{g}}\alpha^{(0)}\right)\left(j\omega+v_{\mathrm{g}}aN_{\mathrm{p}}^{(0)}+\frac{1}{\tau_{\mathrm{sp}}}\right)^{-1}\\&+v_{\mathrm{g}}a_{\mathrm{p}}\Gamma_{\mathrm{a}}N_{\mathrm{p}}^{(0)}-\Gamma_{\mathrm{a}}v_{\mathrm{g}}g^{(0)}+\frac{1}{\tau_{p}}+\Gamma_{\mathrm{J_{BC}}}v_{\mathrm{g}}\alpha^{(0)}\end{aligned}\right]}. \tag{11a}$$

After properly normalized with the DC response ($\omega=0$), the magnitude $U(\omega)$ of the intrinsic optical response $T_{\mathrm{p}}(\omega)$ in the logarithmic scale is defined as

$$U(\omega)=10\log\left|\frac{T_{\mathrm{p}}(\omega)}{T_{\mathrm{p}}(0)}\right|^2. \tag{11b}$$

The responses $U(\omega)$ in different bias conditions are shown in Fig. 3. In Fig. 3(a), we show the responses under different levels of current injections $i_{\mathrm{B}}^{(0)}$ from 60 to 90 mA at $V_{\mathrm{CB}}^{(0)}=1.6$ V. From Eq. (10b), the relaxation frequency ω_{R} increases positively with the DC photon density $N_{\mathrm{p}}^{(0)}$. Since the larger base current $i_{\mathrm{B}}^{(0)}$ brings about the higher photon

Optics EXPRESS

density $N_p^{(0)}$, the larger ω_R and therefore the higher modulation bandwidth can be obtained, as can be observed in Fig. 3(a). This phenomenon is similar to the current-controlled modulation of DLs, in which the output power (photon density), relaxation resonance frequency, and modulation bandwidth would first increase with the injection current once the threshold is reached. On the other hand, under the high current operation, the photon density in fact

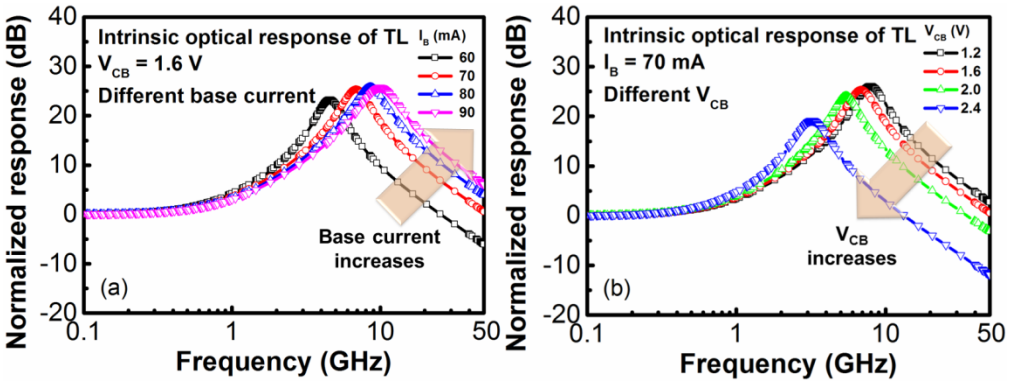

Fig. 3. (a) The magnitude of the intrinsic optical response in the logarithmic scale under different $i_B^{(0)}$ from 60 to 90 mA at $V_{CB}^{(0)}$ = 1.6 V. The modulation bandwidth increases with $i_B^{(0)}$ since the photon density is raised in the cavity. (b) The counterparts at different $V_{CB}^{(0)}$ from 1.2 to 2.4 V ($i_B^{(0)}$ fixed at 70 mA). The modulation bandwidth decreases with $V_{CB}^{(0)}$ due to the less photon density in the cavity.

decreases due to thermal effect for typical DLs. This effect reduces the modulation bandwidth at a high injection level. For TLs, an analogous situation could be also potentially present in the response of voltage-controlled modulation at a high injection current. This phenomenon, however, is not included in our rate-equation model because the power rollover cannot be properly addressed by the linear gain with gain compression. The responses $U(\omega)$ at different $V_{CB}^{(0)}$ from 1.2 to 2.4 V but a fixed $i_B^{(0)}$ of 70 mA are shown in Fig. 3(b). As a result of the larger reverse bias voltage $V_{CB}^{(0)}$, the F-K absorption becomes more significant, and the number of photons becomes smaller. Hence, the modulation bandwidth decreases as $V_{CB}^{(0)}$ increases.

In various bias conditions of TLs considered above, the magnitude $U(\omega)$ of the intrinsic optical response in the logarithmic scale shows an AC enhancement peak more than 20 dB around $\omega = \omega_R$. The enhancement peak can be mainly attributed to the frequency dependency of optical modulation amplitude shown in Eq. (9b), which is similar to the frequency response of carrier densities or frequency modulation in the current modulation of conventional DLs [19]. In the case of TLs, the F-K absorption can directly modulate the photon density and bring a frequency zero ($j\omega$) to the numerator of Eq. (9b), which then leads to the large AC peak. This very prominent peak in the modulation response, however, was seldom observed experimentally. Next, a theoretical model composed of the intrinsic optical response and an electrical transfer function fed back by this optical response is proposed to explain the correct behavior of voltage modulation in TLs.

4. Small-signal electrical model

The modulation bandwidth of optical devices is limited by the parasitic effect of electrical circuits due to the geometry of devices. Generalizing the small-signal circuit of the hybrid

Optics EXPRESS

π model for HBTs, we illustrate the counterpart of TLs for voltage-controlled modulation in Fig. 4. In this model, R_π and C_π are the input resistance and capacitance as looking into the base, respectively; R_μ and C_μ are those due to the reversely-biased BC junction; and R_0 is a resistance due to the Early effect. An additional current source i_{add} resulted from the F-K absorption in the BC junction is incorporated in this electrical model. The parameters R_{E} and

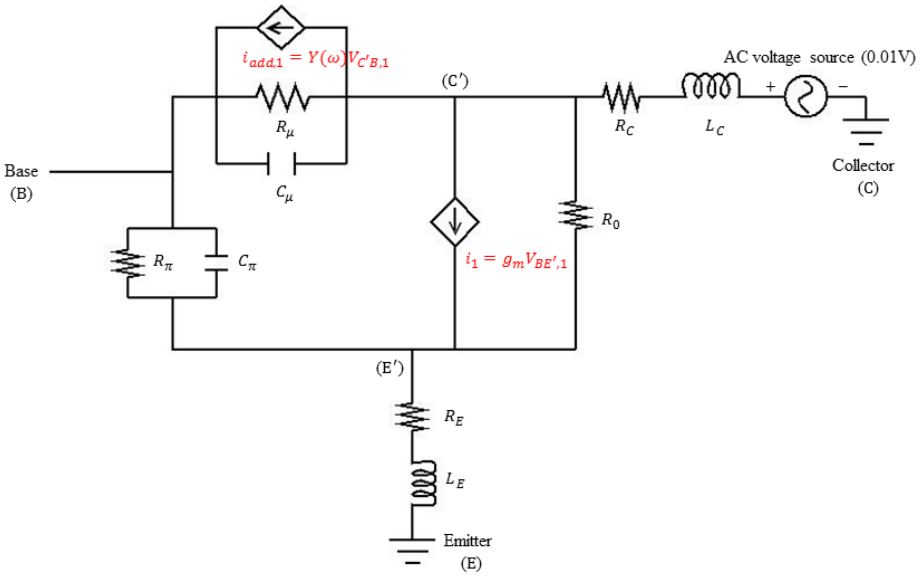

Fig. 4. The small-signal circuit of the TL. An additional current source which is resulted from the F-K absorption in the BC junction is incorporated in this electrical model. The admittance corresponding to this additional current can be deduced from rate equations.

L_{E} stand for the parasitic resistance and inductance of the emitter port while R_{C} and L_{C} are the counterparts of the collector port. Due to the common emitter configuration in this study, the emitter is connected to the ground. Because the base current is fixed, the base port can be regarded as open-circuited in the small-signal model. In our electrical circuit model, an AC voltage source with a magnitude of 0.01 V is connected to the external collector port (C) for small-signal modulations. The other parasitic elements are set to typical values of the small-signal model for LETs and TLs [23,24].

The intrinsic optical response $T_{\text{p}}(\omega)$ obtained in previous calculations is in fact the modulation response related to the voltage amplitude $V_{\text{C'B,1}}$ of the internal collector port (C'), namely, $V_{\text{C'B,1}} = V_1$. In practice, what we monitor is the modulation response corresponding to the external voltage $V_{\text{CB,1}}$ rather than that of $V_{\text{C'B,1}}$. Therefore, the overall response $T_{\text{overall}}(\omega)$ which is experimentally observed should be represented as follows:

$$T_{\text{overall}}(\omega) \equiv \frac{N_{\text{p,1}}}{V_{\text{CB,1}}} = \frac{N_{\text{p,1}}}{V_{\text{C'B,1}}} \times \frac{V_{\text{C'B,1}}}{V_{\text{CB,1}}} = T_{\text{p}}(\omega) \times T_{\text{e}}(\omega), \tag{12}$$

where $T_{\text{e}}(\omega) \equiv V_{\text{C'B,1}} / V_{\text{CB,1}}$ is defined as the electrical transfer function which depends on various small-signal resistances as well as capacitances and would be fed back by $T_{\text{p}}(\omega)$. The

Optics EXPRESS

additional current i_{add} can be inferred from the rate equation of carrier density in Eq. (1a) and is expressed as

$$i_{add} = eV_a\eta' \frac{\Gamma_{J_{BC}}}{\Gamma_a} v_g \alpha N_p, \tag{13}$$

where η' is the percentage of carriers surviving from the electron-hole recombination after being generated in the reversely biased BC junction. The small-signal admittance $Y(\omega)$ corresponding to this additional current is then deduced from Eq. (13). Through the small-signal analysis at the sinusoidal steady state, we obtain the relation between the amplitudes $i_{add,1}$ and $V_{C'B,1}$ of the small signals Δi_{add} and $\Delta V_{C'B}$:

$$i_{add,1} = Y(\omega) V_{C'B,1}, \tag{14a}$$

$$\begin{aligned} Y(\omega) &= eV_a\eta' \frac{\Gamma_{J_{BC}}}{\Gamma_a} v_g \left(\frac{\partial \alpha}{\partial V_{C'B}} N_p^{(0)} + \alpha^{(0)} \frac{N_{p,1}}{V_{C'B,1}} \right)_{V_{C'B} \approx V_{C'B}^{(0)}, i_B = i_B^{(0)}} \\ &= eV_a\eta' \frac{\Gamma_{J_{BC}}}{\Gamma_a} v_g \left[KN_p^{(0)} + \alpha^{(0)} T_p(\omega) \right]. \end{aligned} \tag{14b}$$

Equation (14b) indicates that the admittance $Y(\omega)$ depends on the intrinsic optical response $T_p(\omega)$. Through this admittance, $T_p(\omega)$ directly affects the electrical response $T_e(\omega)$ and therefore the overall response $T_{overall}(\omega)$. In Eq. (14b), if the term proportional to response $T_p(\omega)$ dominates, the magnitude of $Y(\omega)$ may follow the dramatic variation of $T_p(\omega)$ shown in Figs. 3(a) and 3(b). Therefore, the magnitude of admittance $Y(\omega)$ would be at its maximum as the magnitude of the intrinsic optical response $T_p(\omega)$ is at its peak, which reduces the magnitude of the internal voltage drop $V_{C'B,1}$ across the BC junction. In other words, the magnitude of the electrical transfer function $T_e(\omega)$ is approximately at its minimum when the intrinsic optical response is at its maximal magnitude if the effects from various resistances and capacitances are relatively minor. In this model of the TL, behavior of the electrical transfer function is therefore subject to the intrinsic optical response. After taking the full circuit model into account, various normalized magnitude responses of voltage modulations for the TL in the logarithmic scale at different bias voltages ($V_{CB}^{(0)}$ = 1.8, 2.0 and 2.2 V) and an injection current $i_B^{(0)}$ of 70 mA are shown in Fig. 5. The resistance of collector is set to 3 ohm. The electrical transfer function $T_e(\omega)$ is in fact sensitive to this resistance, and this issue will be addressed next. As the magnitude of the admittance is maximal, the magnitude of the voltage drop across the admittance would be minimal. The smallest magnitude of the electrical transfer function $T_e(\omega)$ is reached under such circumstances. After the intrinsic optical response and small-signal circuit model are taken into account simultaneously, the relatively flat magnitude response of $T_{overall}(\omega)$ as compared to $T_p(\omega)$ can be observed. On the other hand, the electrical transfer function $T_e(\omega)$ decreases as the reversely biased voltage $V_{CB}^{(0)}$ increases, as can be told from Fig. 5.

The modulation bandwidth of voltage modulation is limited by the parasitic effect of electrical circuits, especially by the collector resistance R_C. The normalized magnitude of the electrical transfer functions $T_e(\omega)$ in the logarithmic scale at different collector resistances

Optics EXPRESS

from 3 to 6 ohm are shown in Fig. 6(a), and the corresponding overall optical responses are shown in Fig. 6(b). The bias point is set at $V_{CB}^{(0)} = 2.0\,\text{V}$ and $i_B^{(0)} = 70\,\text{mA}$. From Fig. 6(a), as the collector resistance increases, the magnitude of the voltage drop in the BC junction decreases, and therefore the magnitude to electrical transfer function $T_e(\omega)$ is significantly reduced. As a result, the overall optical response $T_{overall}(\omega)$ of the TL is sensitive to collector resistance which is related to geometry and material of device, as can be told from the smaller modulation bandwidth at the larger R_C shown in Fig. 6(b). Therefore, there would be a trade-off between the modulation bandwidth and flat response due to the collector resistance.

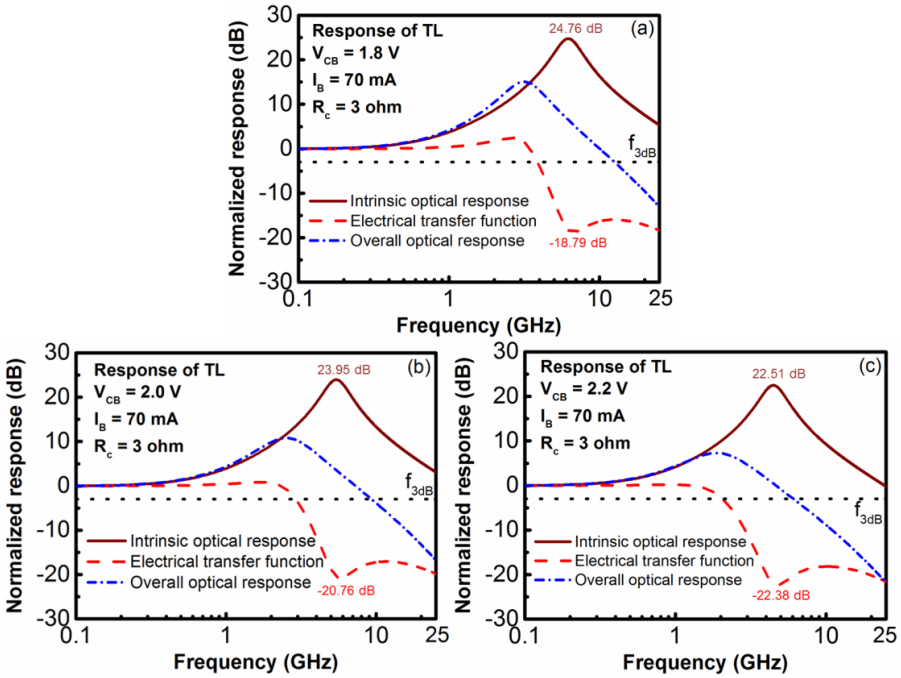

Fig. 5. The comparison among various responses related to the voltage-controlled modulations of the TL at a $V_{CB}^{(0)}$ of (a) 1.8 V, (b) 2 V, and (c) 2.2 V. The magnitude of the electrical transfer function is minimal as the magnitude of the intrinsic optical response is at its peak.

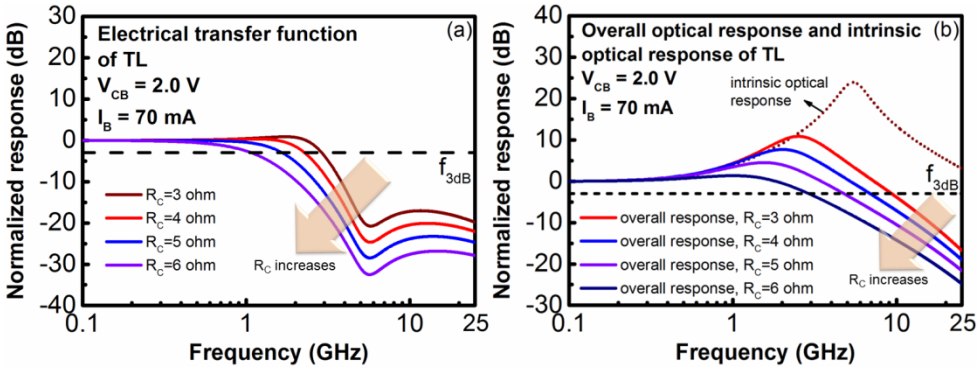

Fig. 6. (a) The electrical transfer function $T_e(\omega)$ and (b) overall response $T_{overall}(\omega)$ at different collector resistances R_C. In the TL, the response $T_{overall}(\omega)$ is sensitive to the collector resistance. As the collector resistance increases, its normalized magnitude decreases but becomes relatively flat.

Optics EXPRESS

5. Conclusion

Compared with conventional DLs, the TL can additionally provide the voltage-controlled modulation due to effect of F-K absorption. On the other hand, the theoretical model merely based on photon-carrier rate equations which incorporate various F-K effects leads to a huge AC enhancement peak on the voltage-controlled modulation response. This phenomenon is not consistent with the relatively flat response observed in the previous experiment. A theoretical model including not only the intrinsic optical characteristics but also an electrical transfer function fed back by optical responses is necessary to explain the correct behaviors of voltage-controlled modulation assisted by the F-K absorption.

Funding

Ministry of Science and Technology of Taiwan (MOST of Taiwan) (MOST 102-2221-E-002-192-MY3, MOST 104-2622-E-002-024-CC3, MOST 104-2622-E-002-032-CC2, MOST 104-2218-E-005-004).

184.96.152.32 {ts '2018-08-01 20:53:05'}